Bulgarian Chemical Communications, Volume 52, Issue 4 (pp. 509-518) 2020 *DOI: 10.34049/bcc.52.4.MP02*

On the potential of integrating extraction with nanofiltration for separating and concentrating polyphenols from plant materials

I. Tsibranska[1*], E. Simeonov[2]

[1]*Institute of Chemical Engineering, Bulgarian Academy of Sciences, Acad. G. Bonchev Str. Bl. 103, 1113 Sofia, Bulgaria*

[2]*Dept. of Chemical Engineering, University of Chemical Technology and Metallurgy, 8 Kl. Ohridski Blvd., 1756 Sofia, Bulgaria*

Received October 3, 2020; Revised October 20, 2020

A green integrated process of solid–liquid extraction and nanofiltration is modeled and numerically investigated considering the separation and concentration of polyphenols from plant extracts. The integrated operation is studied in view of solvent reuse, processing time and degree of concentration. A considerable shortening of the total processing time and reducing of the organic solvent volume is predicted together with high yield and favorable permeate flux. The study is based on extraction kinetics and nanofiltration data for three systems: *Sideritis scardica* × *Sideritis syriaca* – 80% EtOH; *Geranium sanguineum L* – 70% EtOH; and *Cotinus coggygria L.* – 50% EtOH. Over 97% of extractable solute is reached within up to 2 times shorter extraction time; a degree of concentration above 3.7 times in the final product is achieved at 74% solvent recovery.

Keywords: Process integration, modelling, green solid-liquid extraction, polyphenols, nanofiltration.

INTRODUCTION

Plant-derived polyphenols are strong antioxidants with numerous health benefit effects. Their practical utilization implies extraction and further separation/concentration of the phenolic content, the nanolfiltration being recognized as an effective method for the latter. Each one of the processes – solid-liquid extraction (SLE) and membrane filtration – has been investigated in view of optimal operating conditions. Possibilities for intensification of the polyphenols extraction from the solid material are discussed [1] including ultrasound/microwave-assisted extraction [2-4] or supercritical fluid extraction [5]. For a number of industrially important applications integrated membrane processes are proposed [6, 7], because they allow both improved and low-energy separation solvent-extract. In particular, nanofiltration has been intensively investigated for concentration and fractionation of bioactive compounds such as soluble phenolics by selecting a sequence of membranes with suitable molecular weight cut-off (MWCO) in the range of 150–1000 Da [8]. Regarding the composition of the extract, neither extraction nor nanofiltration is selective enough on their own. Their joint use gives satisfactory results when the composition of the extract is valuable and the solvent used is favorable for high value-added molecules, such as polyphenols antioxidants [9-11]. Over the years, the interest in the successive use of the two unit operations is shown in a great number of publications, including optimizing the extraction-nanofiltration process as a whole [3, 4, 12, 13]. The advantages of the latter are demonstrated in terms of green methodology, avoiding high temperatures and toxic solvents, and providing polyphenols recovery from the plant material together with solvent amount reduction. In the search of the final goal to obtain small volumes, concentrated and rich in polyphenols, and to restore an essential part of the solvent for reuse in a subsequent extraction, an integrated extraction-nanofiltration process is expected to reveal a greater potential while preserving the high quality of the extracts [12, 14]. The estimation of the integrated process as possible comprises information about the solvent, the extraction kinetics and the process of transfer across the membrane.

Solvent

The appropriate solvent for both steps of the integrated process is determined by the yield and selectivity to a compound or a group of target compounds, as well as sufficient solubility for the dissolved components over the entire range of concentrations (to prevent precipitation) and non-disruptive effect on the membrane structure. The problem may be significant in extracts containing compounds with a high molecular weight distribution profile and very different solubility. It may lead to uncontrollable flux decline, related to

* To whom all correspondence should be sent:
E-mail: tsibranska@yahoo.com

increased viscosity and oversaturation of higher molecular weight polyphenols at high concentration factors.

Extraction kinetics

Kinetic investigations give essential information about the required time of extraction, as well as on the governing mass transfer mechanism. The appropriate extraction time to approach equilibrium, resp. the range of low variability of the TP yield (the plateau of the kinetic curve) has to be comparable with the time for nanofiltration (needed to achieve a certain degree of concentration) in order to facilitate the integration of the two processes into a single system. In fact, the combination between extraction time and different intensification approaches (temperature, ultrasound- or microwave assistance) is important for the composition and quality of the extract, as well as for the economic feasibility of the process [12]. In general, extraction under agitation is an effective technique for polyphenols extraction because of better hydrodynamic conditions in the extraction vessel and reduced external mass transfer. The mechanisms of mass transfer have been investigated in detail, including the effect of variable rate parameters, particle size evolution and polydispersity [15-18]. Extraction time increases with particle size and, in the presence of large particle size distribution, the larger particles act in the direction of extended both kinetic curve and extraction time [12]. The solute concentration, leaving the extractor vessel, has to be reliably predicted by the kinetic model in order to facilitate the calculations in the NF step, where the value and composition of the feed are very important.

Transport mechanisms across the membrane

High rejections, reasonable values and stability of the permeate flux are required within a predetermined range of feed concentrations, the fouling behavior and mass transfer coefficients being an important source of information [12, 19, 21]. Typical values in the order of 10 l/(m^2 s) are reported for permeate fluxes when concentrating polyphenols containing natural extracts. Rejections over 90% are required in view of the quality of solvent recovery and its possible multiple reuse. Based on the statistical adequacy of the experimental flux *vs* time data regarding the four basic fouling models, the cake layer formation is found as the predominant mechanism, usually followed by the intermediary, standard or complete pore blocking. Mass transfer coefficients in the order of 10^{-5} to 10^{-6} m.s^{-1} are reported for natural antioxidants such as polyphenols extracted from different natural sources [19, 20, 22, 23].

Potential of the integrated SLE-NF separation process

The integration is viewed as a coupling of two unit processes (extraction and nanofiltration, extraction and adsorption, etc.) into a single system (ex. within a common recirculation loop), Fig. 1.

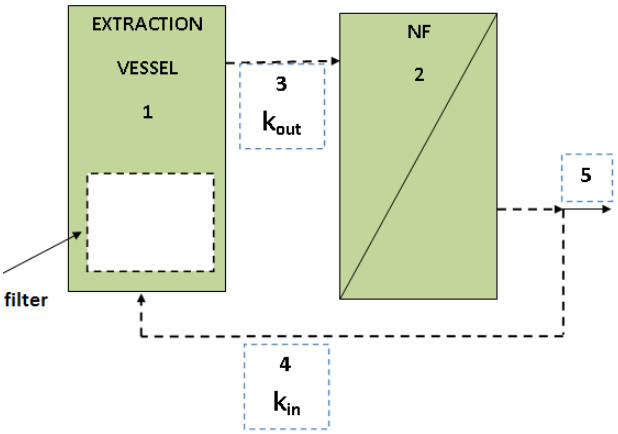

Fig. 1. Schematic representation of the integrated process.

Positive results for integration of solid-liquid extraction with adsorption are recently reported aimed at selective recovery of antioxidant phenolics from chicory grounds [24]. In this case the integration enables simultaneous extraction of phenolics and their purification in a single operation. The comparison with a conventional process of successive extraction and adsorption is in favor of the integrated one because of the higher TP recovery obtained at lower energy consumption [24]. The main purpose of the integration is to achieve better performance than any of the component parts, as weaknesses in certain processes can be reduced by other processes in the integrated system [25]. Though examples for integrated extraction-membrane filtration processes can be found in literature [26, 27], there is little existing experience regarding the principles for integration of the two separation processes, i.e. the simultaneous extraction of phenolics and separation from the solvent in a single system.

The integration of two batch processes is strongly dependent on time, which has to be optimized within the requirements for maximum polyphenols recovery; the latter comprises almost full extraction from the raw material and high solute concentrations in the obtained retentate. The total processing time has to enable high values of extracted polyphenols to be achieved, reuse of the

solvent and full utilization of the raw material, as well as concentrated phenolic content in the final product. For the NF cell operation, it is important to maintain a limited range of variations of the entering (feed) concentrations. The number of recirculated volumes during the integrated extraction-nanofiltration process has to assure values of extracted polyphenols per gram of solid, near the maximum available in the solid to be obtained. The last step (concentration mode) is relevant for the quality and bioactive properties of the final product.

The present study is focused on the potential of integrating solid-liquid extraction with nanofiltration for separating and concentrating polyphenols from plant extracts. The integrated process is investigated in view of three important characteristics - solvent reuse, processing time and degree of concentration.

EXPERIMENTAL

Successive extraction and nanofiltration

The investigation is based on own data for three experimental systems, for which optimal solvent and extraction conditions were found and reported previously [9, 10, 17, 33]. They represent differently fast extraction kinetics, as well as different phenolic contents. The batch kinetic curves shown in Fig. 2 are calculated with the parameter values from Table 1, where data for the three systems, obtained from successive extraction and nanofiltration, are presented.

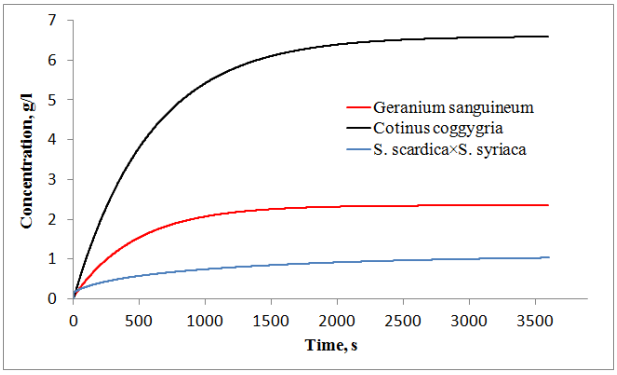

Fig. 2. Batch extraction kinetic curves calculated with the data in Table 1.

System 1 - The genus *Sideritis* L. comprises more than 150 species occurring mainly in the Mediterranean area and the Balkan Peninsula, the selected hybrids *S. scardica*×*S. syriaca* being cultivated since 20 years [28]. The valuable phytochemical content of the plant is utilized either as the traditional remedy tea, or as alcoholic extract with high antioxidant, anti-inflammatory and anti-rheumatic properties. The antioxidant activity is mainly attributed to the flavonoids and phenylpropanoid glycosides content of the plant. Under conventional batch extraction with EtOH 16.4 mg TP/g (solid) were obtained after 2.5 h of extraction, the maximum obtainable after 24 h being 17.5 mg/g solid [17].

Table 1. – Extraction and nanofiltration conditions

EXTRACTION					
No	Solute	Extraction system,	Extraction conditions	Extraction kinetics	Method of analysis
1	TP	*Sideritis scardica*× *Sideritis syriaca* – 80% EtOH [10,17]	LSR 15:1 $2r_0$ $4\cdot10^{-5}$ m T 20 °C	Time 2.5 h D_e $2.5\cdot10^{-14}$m^2/s C_l=1.13 mg/l	Spectrophotometric [32] Gallic acid equivalent Calibration curve [10,17]
2	TP	*Geranium sanguineum L.*- 70% EtOH [33]	LSR 30:1 $2r_0$ 4-$8\cdot10^{-4}$ m T 20 °C	Time 2 h D_e $1.17\cdot10^{-10}$m^2/s C_l=2.37 mg/l	Spectrophotometric [34] Gallic acid equivalent Calibration curve [35]
3	TT	*Cotinus coggygria L.*- 50% EtOH [9]	LSR 30:1 $2r_0$ $3\cdot10^{-4}$ m T 40 °C	Time 2 h D_e $1.90\cdot10^{-11}$m^2/s C_l=6.86 mg/l	Titrimetric [16]
NANOFILTRATION					
No	TMP bar	MWCO Da	J l/(m^2.h)	R_{obs} -	V_p/V_f -
1	20	300	7.3	0.98	0.77
2	30	200	10.0	0.997	0.27
3	20	300	9.0	0.91	0.25

Using ultrasound-assisted extraction (UAE) and cross-flow filtration the total processing time for system 1 in sequential operation mode was reduced to 2.5 h, including 1 h for each of the extraction and NF steps and 0.5 h between them for separation of the solid phase [12]. UAE enabled the maximum amount extracted for 24 h to be obtained within 1 h.

System 2 - The phenol compounds, especially the flavonoids from *Geranium* spp. were reported to exhibit antiviral, antitumor, hepatoprotective, anti-inflammatory, anticancer and immune-stimulant effects. The content of flavonol and flavone glycosides and aglycones in the extracts of *Geranium sanguineum* L. was studied in detail by HPLC [29]. The phytochemical screening of the water extracts (initial, after MF, UF and NF process) showed the presence of flavonoids, reducing sugars, terpenoids, saponins and aminoacids [30]. A potential for concentrating by membrane filtration of the polyphenolic content was demonstrated.

System 3 - *Cotinus coggygria* is a well-known medicinal plant source of high-quality polyphenolic compounds with rich biological activity - antiatherogenic, antioxidant, anti-inflammatory, cardioprotective, antimicrobial, anticarcinogenic and neuroprotective [31]. Ethanolic extracts of *Cotinus coggygria* dry leaves are rich in total phenols, total flavonoids, rutin and tannins. Concentration by NF allows retaining the majority of valuable compounds, the dead-end filtration runs being subject to significant fouling and flux decrease. The data given in Table 1 correspond to the average permeate flux after 4 h of filtration.

Nanomembranes Duramem with low MWCO (200-300 Da) were chosen in view of high rejections and solvent recovery. The filtration data in Table 1 refer to a stirred laboratory NF cell (METcell, Evonic MET LTD, UK) with bottom-placed membrane (effective surface area A=54 cm^2), working volume up to 200 ml, magnetic stirrer close to the membrane surface in order to minimize the concentration polarization effect and stirring speed of 300 rpm.

Integrated extraction-nanofiltration process

The best processing time obtained from the sequential SLE-NF operation (ex. 2.5 h) [12] was used as a time frame for the integrated process, including solvent reuse. Recirculation of the recovered solvent is expected to give shorter extraction time and more complete extraction of the solute for the same initial solvent volume. The three systems in Table 1 have different extraction kinetics, but due to the appropriate choice of solid size and respective intraparticle resistance, the extraction time was reduced to a 2-2.5 h interval. Low concentrations and a narrow range of variation in both the extraction and NF vessels were searched for as favorable in view of higher concentration gradient during extraction and lower susceptibility to fouling during nanofiltration. The criterion for maximum recovery of polyphenols from the plant materials was followed together with high degree of concentration in the final retentate. The latter was achieved by a NF step alone (within the same total processing time), when only concentrating of the solution proceeds.

The model of the integrated extraction-nanofiltration process follows the schematic representation of Fig. 1, where extraction and nanofiltration are carried out separately and are connected in a recirculation loop (lines 3 and 4). When the final step for separating the solvent and concentrating the valuable compounds proceeds, line 4 is excluded and the operation follows lines 3 and 5.

Extraction model

The solid phase extraction is described as a diffusion process with constant effective diffusivity D_e in the particles:

$$\frac{\partial C}{\partial t} = D_e \frac{1}{r^\alpha} \frac{\partial}{\partial r}\left(r^\alpha \cdot \frac{\partial C}{\partial r}\right) \qquad (1)$$

For spherical particles the form factor α=2 and the boundary condition at r=0 accounts for the central symmetry of the concentration profile $C(r,t)$ in the particle:

$$\text{t>0, r=0, } \left.\frac{\partial C}{\partial r}\right|_{r=0} = 0 \qquad (1.1)$$

The second boundary condition at the solid/liquid interface includes the external mass transfer in the fluid film around the particle, k_f being the rate coefficient.

$$\text{t>0, r=R, } \qquad D_e \left.\frac{\partial C}{\partial r}\right|_R = k_f(C|_R - C_l) \qquad (1.2)$$

Usually conditions for eliminating the external mass transfer are searched for and experimentally proven for stirrer speeds above 320 min^{-1} (system 3) [9].

The liquid phase concentration $C_l(t)$ is calculated from the mass balance in the extraction vessel:

$$\frac{\partial C_l}{\partial t} = -\frac{V_s}{V_l}\frac{d\langle C\rangle}{dt} - k_{out}\dot{V}C_l + k_{in}v_y A C_p \qquad (2)$$

The latter runs under intensive agitation, so perfect mixing conditions are supposed in the model and homogeneous concentration $C_l(t)$ within the liquid volume V_l. The volume-averaged solid phase concentration is derived from eq. (1) as follows:

$$\frac{d\langle C\rangle}{dt} = \frac{3}{R^3}\int_0^R \frac{dC}{dt} r^2 dr = \frac{3}{R^3}\int_0^R D_e \frac{1}{r^2}\frac{\partial}{\partial r}\left(r^2\frac{\partial C}{\partial r}\right) r^2 dr \quad (3)$$
$$= \frac{3}{R^3} D_e \left(r^2\frac{\partial C}{\partial r}\right)\Big|_0^R = \frac{3}{R} D_e \frac{\partial C}{\partial r}\Big|_R$$

According to the boundary condition (1.2), it is calculated as:

$$\frac{d\langle C\rangle}{dt} = \frac{3}{R} k_f \left(C\big|_R - C_l\right) \quad (4)$$

Eq. (2) includes the outlet and inlet lines 3 and 4 (Fig. 1), described by the switch on/off keys k_{out} and k_{in}, which take the values of "1" and "0", respectively. Further calculations use the presumption of constant volume V_l, so the outgoing flow rate $\dot{V}$ is set equal to the permeate flow rate $v_y A$. As the permeate flux is a characteristic of the membrane separation, higher flow rate during the simultaneous extraction-nanofiltration operation can be realized by increasing the membrane area (A). The solute concentration in the permeate C_p, appearing in the last term of eq. (2), is calculated from the mass balance of the NF cell.

The initial conditions for solving eqs. (1) and (2) suppose a pure solvent and known initial solute concentration in the solid:

$$t=0,\ 0\le r\le R\ C=C_0,\ C_l=0. \quad (5)$$

Nanofiltration model

The model of the stirred NF cell supposes perfect mixing conditions in the bulk and concentration polarization in the boundary layer to the membrane, accounting for the true rejections and flux decline. When observed, the latter is used as an experimentally defined function of the time of filtration or the volume-averaged retentate concentration. The effect of the permeate concentration and its increase during repeated permeate reuse as solvent is also considered.

The mass transfer in the boundary layer adjacent to the membrane in a dead-end stirred filtration cell is viewed as unsteady one-dimensional problem with a convective flow $v_y C$ directed normal to the membrane and diffusion flow $D_{AB}\frac{\partial c}{\partial y}$ back to the bulk:

$$\frac{\partial c}{\partial t} = D_{AB}\frac{\partial^2 c}{\partial y^2} - v_y \frac{\partial c}{\partial y} \quad (6)$$

The boundary condition at the membrane surface (y=0) accounts for both convective and diffusional mass transfer:

$$0 = D_{AB}\frac{\partial c}{\partial y}\Big|_{y=0} + v_y\left(c_{y=0} - C_p\right) \quad (6a)$$

The true rejection coefficient is used to express the permeate concentration:

$$R_i = 1 - \frac{C_p}{C_m} = 1 - \frac{C_p}{c_{y=0}} \text{ or } C_p = C_{y=0}(1-R_i). \quad (6b)$$

Inserted in equation (6a), the boundary condition at the membrane surface becomes:

$$0 = D_{AB}\frac{\partial c}{\partial y}\Big|_{y=0} + v_y c_{y=0} R_i \quad (7)$$

In the second boundary condition the bulk concentration in the filtration cell was used:

$$c_{y=\delta} = C_r \quad (8)$$

The latter is calculated from the mass balance of the filtration cell:

$$\frac{d(VC_r)}{dt} = -v_y A C_\mathrm{p} + k_{out}\dot{V}C_l = -v_y Ac|_{y=0}(1 - R_i) + k_{out}\dot{V}C_l \quad (9a)$$

$\frac{dV}{dt} = -v_y A + k_{out}\dot{V}$ being the change in the liquid volume, eq. (9a) is transformed to:

$$\frac{dC_r}{dt} = \frac{k_{out}\dot{V}(C_l - C_r) + v_y A\left(C_r - c|_{y=0}(1-R_j)\right)}{V} \quad (9)$$

thus allowing the retentate concentration C_r in the NF cell to be calculated.

When a variable flux case is observed, the experimentally obtained $v_y(t)$ is directly used in eqs. (6) to (9), or after recalculation, in the function of the bulk fluid concentration $v_y(C_r)$.

RESULTS AND DISCUSSION

Effect of the number of recirculated volumes

Fig. 3 illustrates the effect of the multiple solvent recycling on the amount extracted within 2.5 h as compared to the conventional batch extraction.

The initial liquid/solid ratio 15:1 was recommended from previous results (system 1, Table 1). When results for different recycling volumes are compared with batch extraction, the latter is calculated using liquid volume equal to the sum of the recycled volumes plus the initial one. The TP concentration in the recirculating flow is low, equal to the permeate concentration C_p (see

Table 1), while pure solvent was used in the case of conventional extraction.

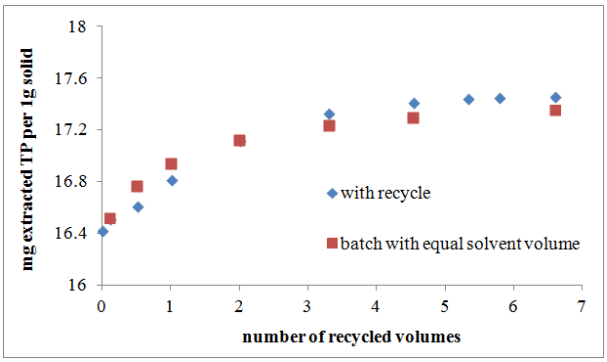

Fig. 3. Effect of the number of recycled volumes of solvent on the amount extracted – calculated results.

Despite this difference, increasing the number of permeate volumes reused, the maximum of extractable TP is approached, the results being comparable or even better than the respective conventional extraction with a larger solvent volume. Experimental confirmation for the suitability of the permeate as a solvent for multiple use is reported for rosmarinic acid from lemon balm [5], where threefold extraction with pure solvent and with NF permeate were compared; similar results are obtained, the difference being in favor of the permeate as solvent. In the presence of over 99% TP rejection (R_i=0.99) the model supposes almost pure solvent, which is not necessarily true in practice, considering the multicomponent composition of the natural extracts. In the particular case of system 1, Table 1, 99.7% of the TP are extracted, the latter being achievable by batch extraction with 6.6 times greater volume of solvent.

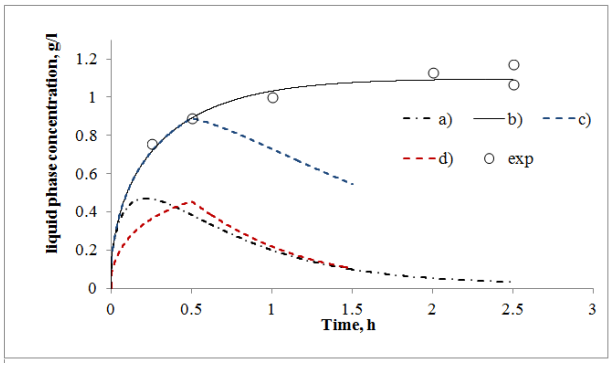

Fig. 4. Calculated bulk TP concentration evolution in the extractor (system 1, LSR 15:1): case a) with recycle; case b) without recycle; case c) without recycle until 80% of the batch plateau, then recycle switched on; case d) 30 min batch extraction (LSR 30:1) + 1 h with recycle (LSR 15:1).

System 1 used powdered solid and the gain of over 6.7% as compared to the batch extraction is not impressive, but it is expected to be higher in cases of slower kinetics (ex. larger particle size) and stronger influence of the liquid to solid ratio.

The evolution of the liquid phase concentration in the extraction vessel is illustrated in Fig. 4, where also the batch extraction curve and the agreement with the experimental points can be seen (Fig. 4, case b). The same kinetic data were used for the rest of the calculations. The corresponding liquid phase profile for extraction with solvent recycle is given in Fig. 4, line a). The latter illustrates also the feed concentration input to the NF vessel. The recirculation case provides operation under lower concentrations and narrower range of their variation for both the extraction and the NF units. The recycle can be used to increase the degree of extraction and to reduce the overall time of the process. Results shown in Fig. 5 illustrate the comparison of different extraction-nanofiltration modes. First conventional extraction was coupled to nanofiltration at different moments of the extraction (C_l=70, 80, 90% of the batch curve plateau) and performed until overall time of 2.5 h. The resulting amounts extracted are shown in Fig. 5 and the concentration evolution in the extraction vessel looks like line c) and d) in Fig. 4.

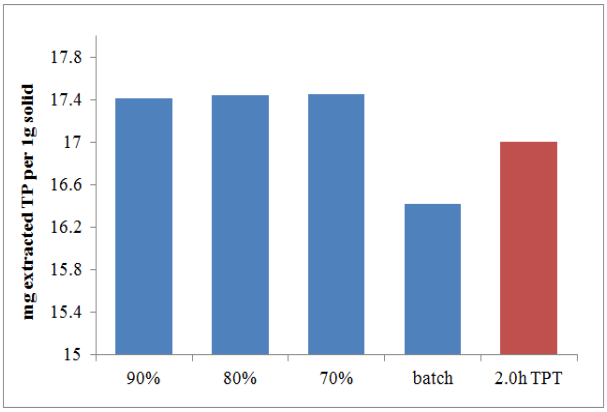

Fig. 5. Calculated amount extracted for different extraction-nanofiltration modes: recycle switched on at C_l=70, 80, 90% of the batch curve plateau; batch; conditions corresponding to Fig. 4, case d, total processing time 2 h.

These two examples are chosen among several numerical calculations investigating the potential for shortening the time of the process. The last one - line d) in Fig. 4 – corresponds to a concentration profile close to the one with maximum TP yield (Fig. 4, line a), but the total processing time (including the concentration step by NF) is reduced to 2 h. Thus over 97% of the extractable TP is reached (the last column in Fig. 5) under 1.7-fold reduction of the extraction time. The experimental procedure comprised 30 min extraction with double

LSR to assure higher concentration gradient in the extraction vessel, followed by 1 h of integrated SLE-NF operation with LSR 15:1 (the rest of the volume being transferred to the NF cell). Then a final step of 30 min for concentrating the TP is provided. The initial concentration for this step is 1.2 mg/ml, at the end C_r/C_f=3.72 of TP concentration degree is achieved together with 74% solvent volume recovery.

Effect of the recirculation flow rate and concentration

In all experiments so far the recirculating flow rate was equal to the one leaving the NF cell. Variation of the latter is practically achievable by increasing the membrane area and/or choosing another membrane. The evolution of the liquid phase concentration under two different recirculation flow rates is shown in Fig. 6. They were calculated based on the measured permeate fluxes (Table 1) and the membrane area. As can be seen, within a twofold increase of the recirculation flow rate, the range of variation of the liquid phase concentration is essentially reduced, which is favorable for the NF cell operation. The degrees of extraction for the experiments shown in Fig. 6 are compared with the batch extraction ones (Fig. 7a).

Except for the slowest kinetics case of system (1), the recirculation flow allowed to increase the degree of extraction over the batch one within 1 h of integrated operation, thus revealing potential for further reduction of the total processing time. For these systems extraction over 99% and threefold concentrating by NF could be achieved in less than 1.5 h total processing time (based on 100 ml initial volume). The calculations were performed both with constant and variable concentration in the recirculation flow. In the first case the measured average permeate concentration in the NF cell were used – 0.023 mg/ml, 0.008 mg/ml and 0.617 mg/ml for systems 1, 2 and 3, respectively.

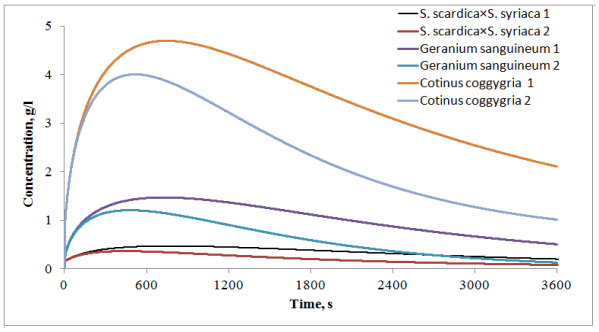

Fig. 6. Effect of the recirculation flow rate on $C_l(t)$: case 1 - permeate fluxes and membrane area according to Table 1; case 2 - twofold increased recirculation flow rate.

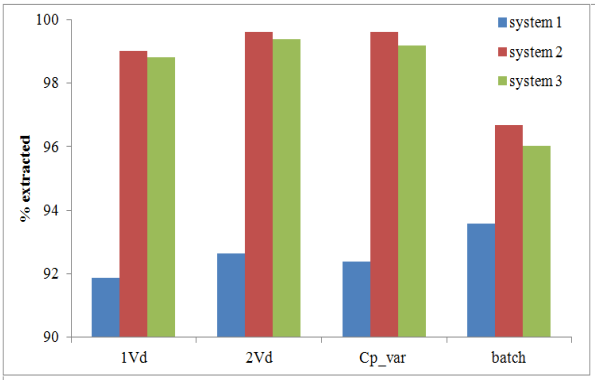

Fig. 7a. Effect of the recirculation flow rate and concentration on the percentage extracted from the solid: 1Vd – permeate fluxes and membrane area according to Table 1 (C_p=const); 2Vd - twofold increased recirculation flow rate (C_p=const); Cp_var – the change in the permeate concentration (line 4, Fig. 1) accounted for; batch results.

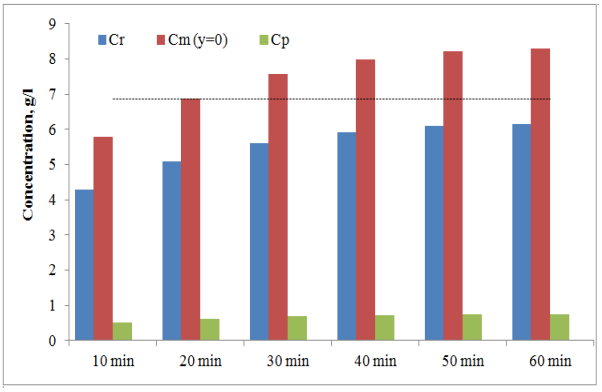

Fig. 7b. Concentration evolution in the NF cell during integrated operation (system 3): columns - calculated retentate, permeate and membrane surface concentrations; dashed line – experimental TP feed concentration in the NF cell, obtained from successive extraction – nanofiltration operation runs.

In the second case variable $C_p(t)$ was used as calculated by the model accounting for the concentration polarization, eqs. (6) to (9). The results are shown as C_{pvar} in Fig. 7a. Due to the narrow concentration range during the integrated operation, no essential effect of the variable concentration is observed. The calculated extracted amount is only slightly less than that with constant C_p and higher recirculation flow rate.

Effect of variable flux and rejection

By selecting the appropriate conditions for narrow concentration variation one can rely on constant permeate flux during the integrated process. For example, in the case referring to line d) in Fig. 4, the TP concentration in the NF cell varied within 0.891 to 0.989 mg/ml during the integrated operation; for comparison, 16.92 mg/g were

extracted for 1.5 h *versus* 16.42 mg/g for 2.5 h batch extraction. The experiments shown in Fig. 6 refer to a wider concentration change in the NF cell, also illustrated in Fig. 7b) for system 3; but the permeate flux should not be less than the one corresponding to the feed concentration in the successive extraction – NF operation. The respective flux values for the three investigated systems and membranes Duramem with different MWCO are shown in Fig. 8a.

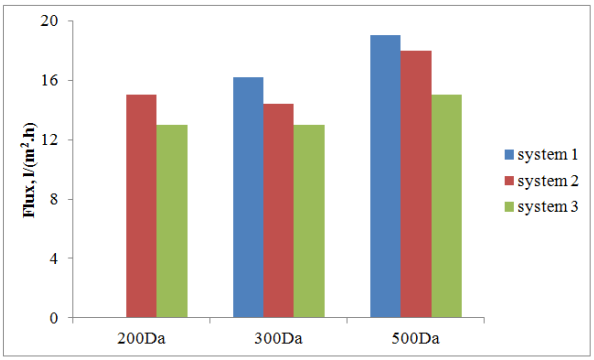

Fig. 8a. Initial permeate flux for different MWCO of the membrane, obtained from experiments with system 1, 2 and 3 in a successive SLE-NF operation.

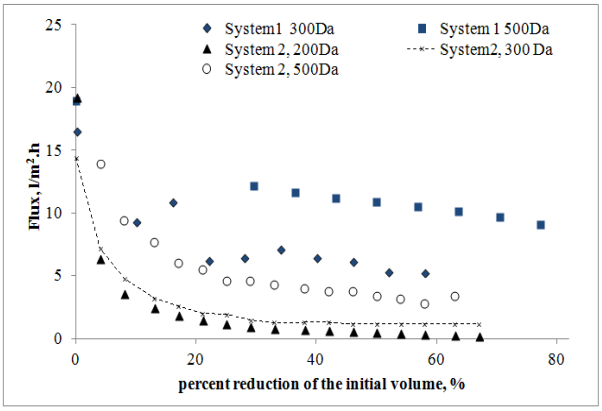

Fig. 8b. Permeate flux *vs* percent reduction of the initial volume for different MWCO (experimental data for systems 1 and 2).

In Fig. 7b concentrations in the NF cell are given (C_p, C_r and C_m) as calculated by the model for integrated SLE-NF operation. The input concentrations for the NF cell are shown in Fig. 6 (*Cotinus coggygria* 2), the output ones being the calculated permeate concentrations (C_p) in Fig. 7b. The averaged permeate concentration agrees with the experimentally measured one (0.618 mg/ml calculated *vs* 0.617mg/ml experimental). The bulk concentration C_r after 1 h of integrated operation does not exceed the feed one (see the dashed line in Fig. 7b) for which NF was initiated with 13 l/(m^2.h) permeate flux. The latter is illustrated in Fig. 8a, according to the data referred for system 3 [9].

The effect of variable flux and rejection is most pronounced during the last step of concentrating the TP content and depends on the composition of the extract and the required degree of concentration (C_r/C_f). Fig. 8b presents the experimentally observed permeate flux decrease for the three systems.

Low but stable permeate flux is reached for system 2 with Duramem 300 until over 60% reduction of the initial volume. For the rest of the cases a gradual flux decrease is observed under dead-end NF operation, thus limiting the achievable degree of concentration.

In case of important flux variation, the latter was included in the model after a mathematical processing of the experimentally observed one. The calculated flux variation has to assure the same average value as the measured one. Example for system 1 is given in Fig. 9a, where the permeated volume *vs* time is shown – experimental and calculated. The average flux for this experiment was 7.34 l/(m^2.h) *vs* 7.13 l/(m^2.h) predicted by the model.

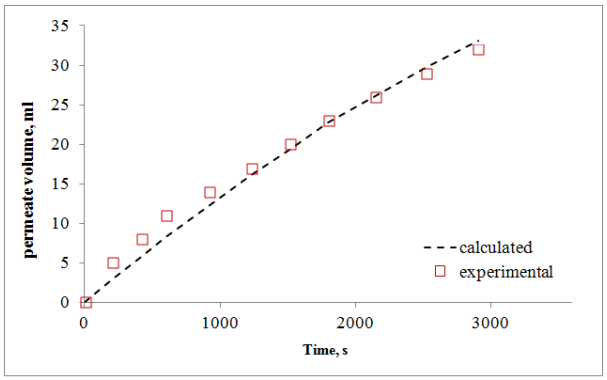

Fig. 9a. Permeate volume *vs* time (system 1).

Rejection was set as constant intrinsic R_i=0.98 according to eq. (6b). Within threefold concentration of the extract an increase in the permeate concentration is expected, due to the concentration polarization (0.023 to 0.086 mg/ml), which results in decreasing observed rejections $R_{obs} = \left(1 - \frac{C_p}{C_f}\right)$ from 0.98 to 0.926. Concentration polarization was accounted for using approximate values of 100 μm boundary layer thickness (δ) and 10^{-9} m^2/s molecular diffusion coefficient (D_{AB}); the order of 10^{-9} m^2/s was chosen as typical for polyphenols in water and ethanol extracts [36]. For these values the evolution of the TP concentrations in the bulk and at the membrane surface (mg/ml), are shown in Fig. 9b.

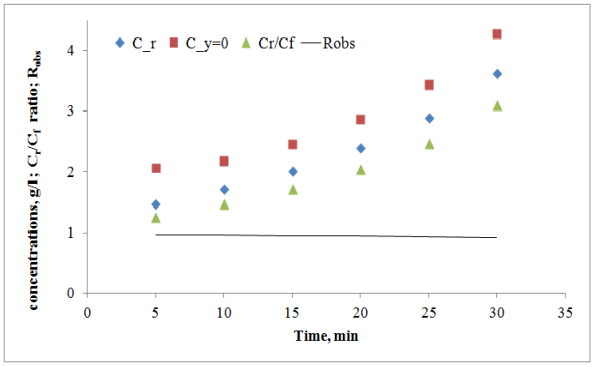

Fig. 9b. Calculated parameters evolution with the time of filtration: retentate side concentrations (g/l), degree of concentration and observed rejections.

CONCLUSIONS

This study is set in the plan of the contemporary environmental trends for exploring natural sources rich in valuable bioactive phenolics. In the same context lies the industrial aspect of the process, including the need to recycle, recover and reuse the solvent. The potential of the latter is investigated in an integrated extraction-nanofiltration process using an appropriate mathematical model and experimental data obtained from the extraction and nanofiltration steps with three different systems. Considerable shortening of the extraction time and reducing of the organic solvent volume is predicted, thus reducing the potential environmental pollution. The integrated process provides higher yield, shorter total processing time, favorable permeate flux. Two solutions were illustrated where the concentrations in the NF cell are maintained at a narrow variation range and/or the permeate flow does not fall below the highest (initial) value recorded for the NF concentration step.

In the first case one can rely on a constant permeate flux during the integrated process. For example, over 97% of the extractable TP was reached with system 1 under 1.7-fold reduction of the extraction time and 20% reduction of the overall processing time by combining three steps: batch extraction, integrated extraction-nanofiltration, final concentrating by NF. At the end a 3.72 fold concentrating of the TP was achieved and 74% of the solvent volume was recovered.

In the second case the integrated extraction-nanofiltration process alone led to reduced extraction time of 1 h (i. e. 2 times shorter). The total processing time including the final concentration step was 1.5 h. The appropriate choice of recirculating flow allows to reduce the range of concentration variation to some extent, the permeate flux being not constant, but also not less than the initial one in the successive extraction – NF operation. High extraction yield is obtained, the advantages over the batch process being more pronounced for faster extraction kinetics, ex. systems 2 and 3.

In fact, the last step of concentrating by nanofiltration offers the main drawbacks, related to considerable flux decrease with increasing retentate concentrations, which also limits the achievable degree of concentration of the final product. Here the experimental observations and the model predictions including variable permeate flux and rejection can help calculating the appropriate final degree of concentration and percent of solvent recovery.

List of Symbols

A membrane area (m^2)
C concentration in the solid (kg/m^3)
C_f feed concentration (kg/m^3)
C_l liquid phase concentration (kg/m^3)
C_0 initial solid phase concentration (kg/m^3)
c concentration in the boundary layer of the NF cell (kg/m^3)
C_p permeate concentration (kg/m^3)
C_r retentate concentration (kg/m^3)
D_{AB} molecular diffusion coefficient (m^2/s)
D_e effective diffusion coefficient (m^2/s)
J permeate flux l/(m^2 h)
k_f external mass transfer coefficient (m/s)
LSR liquid/solid ratio (l/kg)
MWCO molecular weight cut-off (Da)
NF nanofiltration
r radial coordinate (m)
R_{obs} observed rejection (-)
R_j intrinsic rejection (-)
$2R$ particle size (m)
t time (s)
T temperature (°C)
TMP transmembrane pressure (bar)
TP total polyphenols
TT total tannins
V volume liquid in the NF cell (m^3)
V_p/V_f volume permeate/feed ratio (-)
V_s solid phase volume (m^3)
V_l liquid phase volume (m^3)
$\dot{V}$ volumetric flow rate (m^3/s)
v_y permeate flux linear velocity (m/s)
y coordinate normal to the membrane (m)
α form factor (-)
δ boundary layer thickness (m)

REFERENCES

1. A. Oreopoulou, D. Tsimogiannis, V. Oreopoulou, in: Polyphenols in Plants, R. R. Watson (ed.), Academic Press, 2019, p 243.
2. K. Kaderides, L. Papaoikonomou, M. Serafim, A. M. Goula, *Chem. Eng. Process.*, **137**, 1 (2019).
3. R. S. Rabelo, M. T. C. Machado, J. Martínez, M. D. Hubinger, *J. Food Eng.*, **178**, 170 (2016).
4. J. A. A. Meija, G. P. Parpinello, A. Versari, A., C. Conidi, A. Cassano, *Food Bioprod. Process.*, **117**, 74 (2019).

5. G. Peev, P. Penchev, D. Peshev, G. Angelov, *Chem. Eng. Res. Des*., **89**(11), 2236 (2011).
6. I. Tsibranska, B. Tylkowski, in: Integrated membrane operations in the food production, A. Cassano, E. Drioli, (eds.), De Gruyter, 2013, p. 269.
7. C. Conidi, E. Drioli, A. Cassano, *Curr. Opin. Food Sci*., **23**, 149 (2018).
8. B. Tylkowski, M. Nowak, I. Tsibranska, A. Trojanowska, L. Marciniak, R. Garcia Valls, T. Gumi, M. Giamberini, *Curr. Pharm. Design.*, **23**(2), 231 (2017).
9. V. Koleva, E. Simeonov, *Chem. Biochem. Eng. Q*., **28**(4), 545 (2015).
10. B. Tylkowski, I. Tsibranska, R. Kochanov, G. Peev, M. Giamberini, *Food Bioprod. Process.*, **89**(4), 307 (2011).
11. B. Tylkowski, B. Trusheva, V. Bankova, M. Giamberini, G. Peev, A. Nikolova, *J. Memb. Sci.*, **348**(1-2), 124 (2010).
12. A. Trojanowska, I. Tsibranska, D. Dzhonova, M. Wroblewska, M. Haponska, P. Jovancic, V. Marturano, B. Tylkowski, *Chem. Eng. Res. Des.*, **147**, 378 (2019).
13. M. A. Nunes, S. Pawlowski, A. S. Costa, R. C. Alves, M. B. P. Oliveira, S. Velizarov, *Sci. Total Environ*., **652**, 40 (2019).
14. I. Tzibranska, I. Seikova, R. Kochanov, V. Kancheva, G. Peev, in: Nanoscience & Nanotechnology, vol. 9, E. Balabanova, I. Dragieva, (eds.), BAS-NCCNT, Sofia, 2009, p. 210.
15. E. Simeonov, Z. Yaneva, C. Chilev, *Green Process. Synth*., **7**(1), 68 (2018).
16. C. Chilev, V. Koleva, E. Simeonov, *Ind. Eng. Chem. Res*., **53**(15), 6288 (2014).
17. I. Tsibranska, B. Tylkowski, R. Kochanov, K. Alipieva, *Food Bioprod. Process*., **89**(4), 273 (2011).
18. I. Tsibranska, B. Tylkowski, *J. Chem. Technol. Metall*., **51**(5), 489 (2016).
19. I. Dammak, M. A. Neves, H. Nabetani, H. Isoda, S. Sayadi, M. Nakajima, *Food Bioprod. Process*., 94, 342 (2015).
20. A. Giacobbo, A. Moura Bernardes, M. Filipe Rosa, M., de Pinho, *Membranes*, **8**(3), 46 (2018).
21. I. Tsibranska, B. Tylkowski, *Food Bioprod. Process*., **91**(2), 169 (2013).
22. S. Todisco, P. Tallarico, B. Gupta, *Innov. Food Sci. Emerg. Technol*., **3**(3), 255 (2002).
23. C. Li, Y. Ma, H. Li, G. Peng, *Food Sci. Nutr*., **7**, 1884 (2019).
24. D. Pradal, P. Vauchel, S. Decossin, P. Dhulster, K. Dimitrov, *Chem. Eng. Process*., **127**, 83 (2018).
25. W. L. Ang, A. W. Mohammad, N. Hilal, C. P. Leo, *Desalination*, **363**, 2 (2015).
26. I. X. Cerón, R. T. L. Ng, M. El-Halwagi, C. A. Cardona, *J. Food Eng*., **134**, 5 (2014).
27. M. Cissé, F. Vaillant, D. Pallet, M. Dornier, *Food Res. Int*., **44**(9), 2607 (2011).
28. L. Evstatieva, *Annuaire de l'Université de Sofia "St. Kl. Ohridski" Faculté, de Biologie, Livre 2 Botanique*, **97**, 45 (2006).
29. S. Leucuta, L. Vlase, S. Gocan, L. Radu, C. Fodorea, *J. Liq. Chromatogr. Relat. Technol*. **28**(19), 3109 (2005).
30. G. Paun, E. Neagu, A. Tache, G. L. Radu, V. Parvulescu, *Chem. Biochem. Eng. Q*., **25**(4), 453 (2011).
31. V. L. Christova-Bagdassarian, M. S. Atanassova, V. K. Hristova, M. A. Ahmad, *Int. J. Sci. Eng. Res.*, ***7***(2), 1466 (2016).
32. V. L. Singleton, R. Orthofer, R. M. Lamuela-Raventós, *Method Enzymol*., **299**, 152 (1999).
33. E. Simeonov, V. Koleva, *Chem. Biochem. Eng. Q*., **26**(3), 249 (2012).
34. D. Marinova, F. Ribarova, M. Atanassova, *J. Univ. Chem. Technol. Metall*., **40**(3), 255 (2005).
35. E. Simeonov, V. Koleva, G. Nedeva, *J. Univ. Chem. Technol. Metall*., **46**(1), 41 (2011).
36. M. S. Guerrero, J. S. Torres, M. J. Nuñez, *Bioresource Technol.*, **99**(5), 1311 2008.